

Semi-analytical solution of dam-reservoir interaction in the fundamental mode shape

Paulo Marcelo Vieira Ribeiro, Carlos Augusto Elias Melo
and Lineu José Pedroso

*Department of Civil and Environmental Engineering - ENC/UnB
Brasília/DF – Brazil*

Abstract

This paper describes a semi-analytical procedure for solution of dam-reservoir interaction in the fundamental mode shape. The fundamental frequency is solved using a generalized coordinate approach mixed with a wave equation analytical solution for a flexible boundary, resulting in a coupled system equilibrium frequency equation. Pressure field in the fluid domain and fluid added mass are obtained upon the solution of this equation. A full development of the theory will be presented, along with application examples. Results indicate good agreement between finite element solution for the coupled system and the resulting fluid added mass solution. This methodology provides a useful resource for solution of the coupled system and can be readily applied in dam engineering problems.

Keywords: dams, reservoir, fluid-structure interaction, analytical, solution.

1 Introduction

The aim of this work is to evaluate the influence of hydrodynamics pressures in systems with fluid-structure coupling. Two approaches may be used: solutions involving both solid and fluid domain, and representation of fluid effects through added masses along the structure. The added mass technique consists in substituting the hydrodynamic pressures exerted on the structure's face by a set of masses, which are proportionally accelerated as the structure vibrates. This provides an equivalent system which is able to represent the coupling effects for a given mass configuration. The major advantage of this sort of representation is the elimination of an additional step in the solution of the coupled problem, which is the consideration of fluid domain.

The fluid-structure interaction problem involves the determination of structure and fluid responses. However, it is important to emphasize that these responses are not independent. Fluid domain pressure field depends on the structural displacement, which in turn depends on the forces exerted by the fluid on the structure's face. A very efficient solution for this problem consists in determining, for

an imposed structural displacement, the fluid produced pressure field. This provides a possible way to develop analytical solutions for the fluid domain. Numerous solutions that consider compressible and incompressible fluids are available in literature, either for rigid boundaries or flexible boundaries (with an imposed deformed shape along fluid-structure interface). The pressure field produced by these solutions along the fluid-structure interface represents exactly the loads that must be added to the structure, providing the coupling effects between these two systems. The combination between analytical solution for pressure in fluid domain and analytical solution for structural response allows the development of a global solution that provides the effects of fluid produced actions in the structure.

The studies presented below involve the analysis of dynamic systems in generalized coordinates, considering only the structure's fundamental mode shape. The results involving coupled and uncoupled systems with effects of added mass will be compared in order to validate the proposed procedure. The effects produced by the fluid added mass presence will be studied, including its application in practical dam engineering analysis.

2 Literature review

The problem of dam-reservoir interaction has been widely studied in the last decades. The first attempt to solve this problem was made by Westergaard [1]. He considered a dam accelerated at its base as a perfect rigid body with a continuum infinite length reservoir. Because of the perfect rigidity of the dam, its acceleration along the structure was considered constant and equal to the foundation's acceleration. For these conditions, Westergaard found out a solution for the pressure field, which acts on the dam's face when it is under a seismic excitation. These studies demonstrated that fluid pressure had a parabolic shape, being proportional to earthquake acceleration. This is the simplest form of treating the dam-reservoir problem. However this solution has the limitations of not being valid for flexible structures and not considering the fluid compressibility.

Many other researchers determined the hydrodynamics pressure exerted on the dam's face as a result of earthquake ground motions for an incompressible fluid. To determine it using the Finite Element Formulation, a problem in modeling arises for unbounded domains of reservoir. To solve this problem, the unbounded domain should be truncated at a certain distance away from the structure. Zienkiewicz & Newton [2] used the Sommerfeld's radiation boundary condition for the truncating surface; Sharan [3] and Küçükarslan [4] determined numerically other boundary conditions for truncating surface of unbounded fluid domain; Silva & Pedroso [5] determined a solution for this problem using separation of variables technique for the same boundary conditions used for Zienkiewicz & Newton and Sharan & Küçükarslan, and proposed a new boundary condition.

Chopra [6] found out that water compressibility plays an important role in dam-reservoir interaction problems. According to his studies, fluid compressibility can significantly modify the seismic response. Chopra [7] investigated the response of a concrete gravity dam under horizontal earthquake excitation considering interactions effects and water compressibility, and concluded that commonly used simplified analysis, which neglect the interaction between dam and reservoir, and water compressibility, can result in significant errors. Chopra (1978) proposed a methodology in which the above-mentioned considerations were included.

Chopra & Fenves [8, 9] studied a system compound of a concrete gravity dam including the effects of water-foundation-rock interaction and the alluvium, and other sediments that deposit at the bottom of reservoirs. The interaction between the water and the reservoir bottom materials is approximately modeled by a boundary condition that permits partial absorption of hydrodynamic pressure waves at the reservoir bottom. In brief, it was shown that the earthquake response of concrete gravity dam is increased by dam-water interaction, but decreased by reservoir bottom absorption with the magnitude of these effects dependent on the flexibility of the foundation rock, and dam-water interaction and reservoir bottom absorption both have a profound effect on the response of dams to vertical ground motion, but relatively less effect on the response to horizontal ground motion if foundation-rock flexibility is considered.

Many researches, for instance, Saini et al. [10], Chopra & Chakrabarti [11], Hall & Chopra [12], Fenves & Chopra [13], Fok & Chopra [14], and Lotfi et al. [15] studied dam-reservoir interaction problem in the frequency domain considering water compressibility using the Finite Element Method.

Ribeiro [16] proposed a methodology which provides an analytical solution of stress field in concrete gravity dams during earthquakes. This solution was developed taking the Gravity Method as a basis. This method, proposed by the United States Bureau of Reclamation – USBR [17], is designed for static and pseudo-static analysis (dam as a perfect rigid body and fluid incompressible) of concrete gravity dams. Ribeiro combined this solution with the methodology proposed by Chopra [18]. This combination allowed consideration of water compressibility and structural flexibility in the Gravity Method. The achieved results with this methodology are slightly conservative when compared to Chopra's procedure. It was shown that structural flexibility and water compressibility increases the earthquake response of concrete dams.

Silva [19] proposed an analytical formulation using separation of variables technique for the hydrodynamic pressure exerted on the dam's face under seismic excitation, considering structural flexibility and water compressibility. His results indicated a good agreement with the Finite Element Method.

3 Fluid domain analytical solution

Consider the following domain which is governed by the wave equation in two dimensions and represented in Fig. 1, where $S1$, $S2$, $S3$ and $S4$ represent the following boundary conditions:

$$S1 = \left. \frac{\partial p(x, y, t)}{\partial x} \right|_{x=0} = -\rho\phi\ddot{U}_g \quad (1)$$

$$S2 = \left. \frac{\partial p(x, y, t)}{\partial y} \right|_{y=0} = 0 \quad (2)$$

$$S3 = p(x, y, t)|_{x \rightarrow s} = 0 \quad (3)$$

$$S4 = p(x, y, t)|_{y=H} = 0 \quad (4)$$

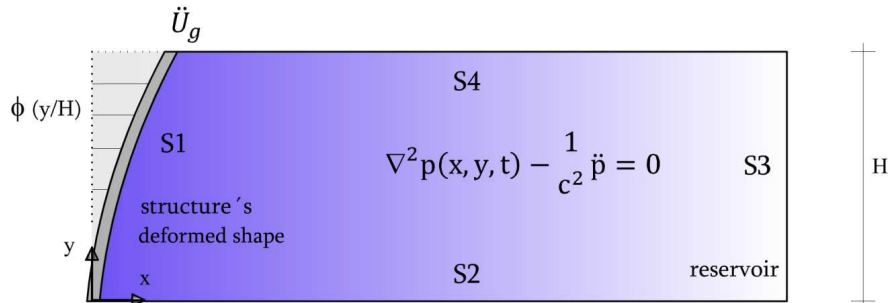


Figure 1: Fluid domain representation with boundary conditions.

and \ddot{U}_g represents the acceleration at the structure's free edge ($y = H$). Silva [19] proposed a solution for this problem where the shape function $\phi(y)$ can be defined as an arbitrary function. This solution considers the fluid compressibility and depends on the frequency of the coupled system (ω).

$$p(x, y) = 2\rho\ddot{U}_g \sum_{n=1}^{\infty} \frac{I_n}{\sqrt{\mu_n^2 - \left(\frac{\omega H}{c}\right)^2}} e^{-\sqrt{\mu_n^2 - \left(\frac{\omega H}{c}\right)^2} \frac{x}{H}} \cos\left(\mu_n \frac{y}{H}\right) \quad (5)$$

$$I_n = \int_0^H \phi\left(\frac{y}{H}\right) \cos\left(\mu_n \frac{y}{H}\right) dy \quad (6)$$

$$\mu_n = \frac{(2n-1)\pi}{2} \quad (7)$$

In the case of analysis that will be developed in this study, the function adopted corresponds to the fundamental deformed shape. Therefore, an analytical solution for the pressure field produced by the structural displacement in the fundamental vibration mode is achieved. The pressure field exerted on the fluid-structure interface can be obtained by setting up $x = 0$ in the above equations. Doing so, we get:

$$p(0, y) = 2\rho\ddot{U}_g \sum_{n=1}^{\infty} \frac{I_n}{\sqrt{\mu_n^2 - \left(\frac{\omega H}{c}\right)^2}} \cos\left(\mu_n \frac{y}{H}\right) \quad (8)$$

which represents the pressure field developed along the fluid-structure interface for a boundary with acceleration proportional to the adopted shape function $\phi(y)$. The latter expression is the starting point for the inclusion of the fluid participation in the dynamic response of the structure. It is important to remember that the parameter $\omega H/c$, called compressibility parameter, is an important indicator in this type of solution (the pressure field suffers important modifications when this parameter varies, as shown in Fig. 2).

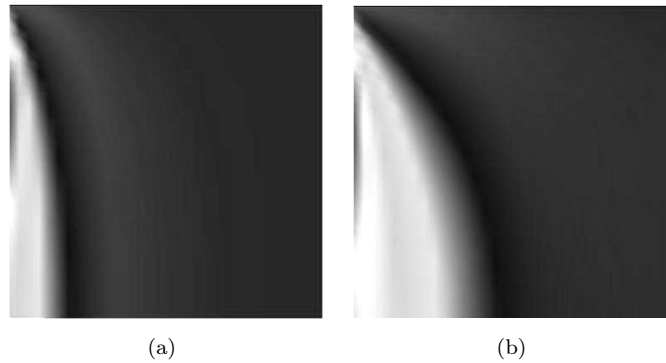


Figure 2: Hidrodinamic pressure field variation along the reservoir for $\omega H/c = 0$ (a) and $\omega H/c = 1$ (b).

The characteristics of the hydrodynamic pressure approaches the behavior of an incompressible fluid as this parameter tends to zero (Fig. 3), resulting in a solution of a flexible boundary in an incompressible fluid. This indicates that the above solution is a general, valid for both compressible and incompressible fluid behavior.

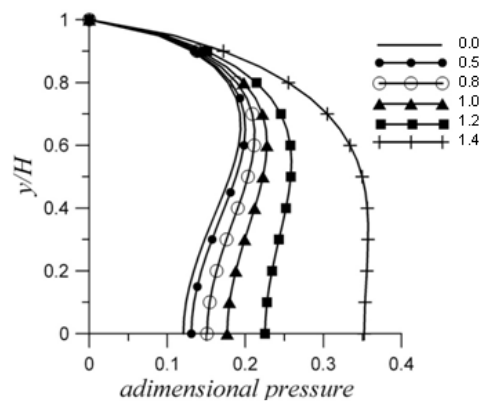


Figure 3: Pressure along fluid-structure interface for $\omega H/c$ parameter variation (fundamental mode).

4 Analytical solution for the structural system

The structural problem is represented by a clamped-free beam, where the generalized properties of the system (mass, stiffness and excitation) for an arbitrary vibration function were derived. Thus, it will

be possible to represent the dynamic response of the model through a single coordinate $X(t)$. This kind of solution will be very useful for the introduction of fluid effects since the analytical solution for this domain was obtained for an imposed frequency (ω) and shape function $\phi(y)$.

Consider the structure below with the arbitrary following parameters: mass per unit length $\mu(y)$, flexural stiffness $EI(y)$ and under a transverse loading $P(y, t)$.

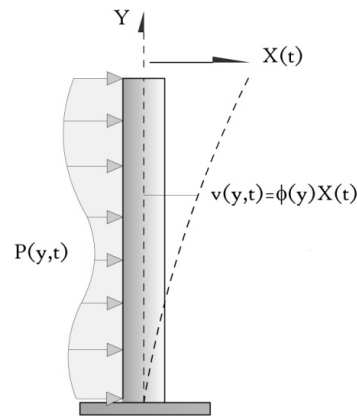


Figure 4: Structural model representation.

where the transverse-displacement response is represented by $v(y, t)$ and is related to the deformation at the top of the beam $X(t)$ by means of an arbitrary shape function $\phi(y)$. Doing so, we get:

$$v(y, t) = \phi(y) X(t) \quad (9)$$

The resistant forces in this system during the structure displacement are given by Inertial Force (Eq. 10) and Internal Bending Moment (Eq. 11):

$$f_i(y, t) = \mu(y) \ddot{v}(y, t) = \mu(y) [\ddot{X}\phi(y)] \quad (10)$$

$$m(y, t) = EI(y) \frac{\partial^2 v}{\partial y^2} = EI(y) \left[X \frac{d^2 \phi(y)}{dy^2} \right] \quad (11)$$

Thus, it is assumed that only bending deformations will occur and the elastic moments developed will be proportional to curvature $\partial^2 v / \partial y^2$. The system's equation of motion can be obtained through the application of the principle of virtual work, equaling the work of internal forces to the work of external forces. The virtual displacement (δv) consistent with structural deformation ϕ is given by:

$$\delta v = \phi(y) \delta X \quad (12)$$

where δX corresponds to an arbitrary virtual displacement in the free edge of the structure. The work of external forces during this virtual displacement is given by:

$$W_e = \int_0^H P(y, t) \delta v \, dy = \delta X \int_0^H P(y, t) \phi(y) \, dy \quad (13)$$

The work of the internal forces (inertia and bending moment) is given by:

$$W_i = \int_0^H f_i(y, t) \delta v \, dy + \int_0^H m(y, t) \delta \frac{\partial^2 v}{\partial y^2} \, dy \quad (14)$$

Substituting the expressions of inertia force (Eq. 10) and internal bending moment (Eq. 11) in the expression above, and remembering that:

$$\delta v = \phi(y) \delta X \quad (15)$$

$$\delta \frac{\partial^2 v}{\partial y^2} = \delta X \frac{d^2 \phi(y)}{dy^2} \quad (16)$$

provides:

$$W_i = \int_0^H \mu(y) [\ddot{X} \phi(y)] \phi(y) \delta X \, dy + \int_0^H EI(y) \left[X \frac{d^2 \phi(y)}{dy^2} \right] \delta X \frac{d^2 \phi(y)}{dy^2} \, dy \quad (17)$$

When simplified, the expression above results in:

$$W_i = \ddot{X} \delta X \int_0^H \mu(y) [\phi(y)]^2 \, dy + X \delta X \int_0^H EI(y) \left[\frac{d^2 \phi(y)}{dy^2} \right]^2 \, dy \quad (18)$$

Equating external work with internal work and dividing the resultant expression by the arbitrary virtual displacement δX , gives:

$$\int_0^H P(y, t) \phi(y) \, dy = \ddot{X} \int_0^H \mu(y) [\phi(y)]^2 \, dy + X \int_0^H EI(y) \left[\frac{d^2 \phi(y)}{dy^2} \right]^2 \, dy \quad (19)$$

Finally, introducing the following notations, we get the Generalized Mass \tilde{M} (Eq. 20), the Generalized stiffness \tilde{K} (Eq. 21), and the Generalized Force \tilde{P} (Eq. 22):

$$\tilde{M} = \int_0^H \mu(y) [\phi(y)]^2 dy \quad (20)$$

$$\tilde{K} = \int_0^H EI(y) \left[\frac{d^2 \phi(y)}{dy^2} \right]^2 dy \quad (21)$$

$$\tilde{P} = \int_0^H P(y, t) \phi(y) dy \quad (22)$$

And substituting these notations in Eq. 19, results in:

$$\tilde{M}\ddot{X} + \tilde{K}X = \tilde{P}(t) \quad (23)$$

This is the system's dynamic equilibrium equation which has a vibration frequency equal to:

$$\omega = \sqrt{\tilde{K}/\tilde{M}} \quad (24)$$

It should be emphasized that the generalized stiffness obtained for this system includes only the effects of bending deformation. Additional effects can be introduced through the modification of this generalized parameter. Damping could also be added to this structure, and in this case it would be more appropriate to express it by damping ratio (ξ). Thus, we have:

$$\tilde{C} = 2\xi\tilde{M}\omega \quad (25)$$

5 Coupled problem analytical solution

The solutions presented above are valid for each isolated domain, both solid and fluid. However, a problem of great interest arises when it is necessary to verify the interaction effects produced between these two systems. In the case of the solution presented for the fluid domain, it is known the pressure field for a particular shape function. This pressure field can be properly added to the structural solution, since it is known the external forces produced by the hydrodynamic interaction. So, we have:

$$P(y, t) = p(0, y) = 2\rho\ddot{X} \sum_{n=1}^{\infty} \frac{I_n}{\sqrt{\mu_n^2 - \left(\frac{\omega H}{c}\right)^2}} \cos\left(\mu_n \frac{y}{H}\right) \quad (26)$$

Where the external forces are associated to the coupled frequency (ω) of the system and depend on the coupled shape function $\phi(y)$ of the structure. It is important to remember that the term \ddot{U}_g was properly substituted by \ddot{X} , since in the coupled system accelerations of the free edge of the structure and of the flexible boundary are equal. Substituting the last equation (Eq. 26) in the generalized force equation (Eq. 22), results in:

$$\tilde{P}(t) = \ddot{X} \int_0^H \left[2\rho \sum_{n=1}^{\infty} \frac{I_n}{\sqrt{\mu_n^2 - \left(\frac{\omega H}{c}\right)^2}} \cos\left(\mu_n \frac{y}{H}\right) \right] \phi(y) dy = \ddot{X} \int_0^H \left[\frac{\beta}{\phi(y)} \right] [\phi(y)]^2 dy \quad (27)$$

It is interesting to note the similarity between the simplified result of this expression and the generalized mass equation in the structural model. We can rewrite the dynamic equilibrium equation of the structure to check the influence of this parameter. Thus:

$$\tilde{M}\ddot{X} + \tilde{K}X + \ddot{X} \int_0^H \left[\frac{\beta}{\phi(y)} \right] [\phi(y)]^2 dy = 0 \quad (28)$$

In this equation, the generalized force expression was placed on its left side, since the hydrodynamic pressures acts in the same direction of the inertia and elastic forces. We can rewrite Eq. (28), noticing that there are two terms along with \ddot{X} . This results in:

$$\left(\tilde{M} + \int_0^H \left[\frac{\beta}{\phi(y)} \right] [\phi(y)]^2 dy \right) \ddot{X} + \tilde{K}X = 0 \quad (29)$$

This equation represents the free-vibration of the structural model with a generalized mass produced by the interaction between fluid and solid domain. Physically, this means that the structure in contact with the fluid presents an additional vibrating mass which is distributed per unit length because the expression for generalized mass can be rewritten as follows:

$$\tilde{M}_{total} = \int_0^H \left\{ \mu(y) + \left[\frac{\beta}{\phi(y)} \right] \right\} [\phi(y)]^2 dy \quad (30)$$

where $\frac{\beta}{\phi(y)}$ represents the added mass per unit length caused by fluid presence.

The new dynamic equilibrium equation of the system is given by:

$$\tilde{M}_{total}\ddot{X} + \tilde{K}X = 0 \quad (31)$$

where it should be remembered that the generalized stiffness parameter is still defined by:

$$\tilde{K} = \int_0^H EI(y) \left[\frac{d^2\phi(y)}{dy^2} \right]^2 dy \quad (32)$$

It is important to remember that the shape function $\phi(y)$ now refers to the coupled system. Therefore, it should be taken great care not to confuse the shape function of the coupled system with the one for the uncoupled system. Similarly, the vibration frequency ω also refers to the coupled system and is given by:

$$\omega = \sqrt{\frac{\tilde{K}}{\tilde{M}_{total}}} \quad (33)$$

This frequency equation, although presented in a simple manner, is not an easy problem to be solved. It should be noted that the frequency is a function of the generalized stiffness, which is a function of the coupled system shape function $\phi(y)$. Also, the system's total mass is a function not only of $\phi(y)$, but also a function of the coupled frequency (ω) of the system. Therefore, this problem defines only one equation and two unknown parameters.

6 Application example 1 – incompressible fluid

In this example a cantilever beam of uniform cross section will be analyzed. By this way, it is intended to validate the afore-mentioned procedure and verify the effects produced by fluid-structure coupling in the fundamental mode. Figure 5 and Table 1 illustrates the structure that will be analyzed and its material and geometrical properties:

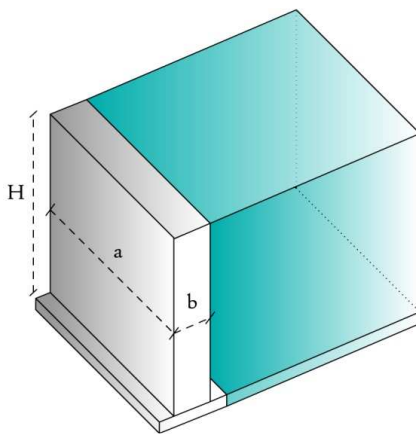


Figure 5: System representation.

Table 1: Geometrical and material properties.

a	1.00 m
b	0.10 m
H	1.00 m
Transverse Young's Modulus (E)	2.10×10^4 MPa
Structural mass density (ρ_e)	2000 kg/m ³
Fluid mass density (ρ_f)	1000 kg/m ³
Fluid sonic velocity (c)	1500 m/s

6.1 Uncoupled solution

For the uncoupled solution, the generalized mass and stiffness defined for the structural domain can be used. The exact fundamental mode shape function for a cantilever beam is given by:

$$\phi(y) = \frac{1}{2} \cosh\left(1.8751 \frac{y}{H}\right) - \frac{1}{2} \cos\left(1.8751 \frac{y}{H}\right) - 0.3670 \sinh\left(1.8751 \frac{y}{H}\right) + 0.3670 \sin\left(1.8751 \frac{y}{H}\right) \quad (34)$$

Substituting the above equation along with system's material and geometrical properties in the generalized parameters gives:

$$\tilde{M} = \int_0^H \mu(y) [\phi(y)]^2 dy = \mu \int_0^H [\phi(y)]^2 dy \cong 0.25\mu H = 5.00 \times 10 \frac{Ns^2}{m} \quad (35)$$

$$\tilde{K} = \int_0^H EI(y) \left[\frac{d^2\phi(y)}{dy^2} \right]^2 dy = EI \int_0^1 \left[\frac{d^2\phi(y)}{dy^2} \right]^2 dy \cong 3.09 \frac{EI}{H^3} = 5.41 \times 10^6 \frac{N}{m} \quad (36)$$

$$\omega = \sqrt{\tilde{K}/\tilde{M}} = 328.94 \frac{rad}{s} \quad (37)$$

The last equation represents the fundamental frequency for uncoupled system.

6.2 Coupled solution

For calculation of generalized parameters including coupling effects, a previous knowledge of the shape function $\phi(y)$ of the system is needed. The exact solution for the uncoupled fundamental mode shape is known. Therefore, we will assume that in the coupled system the fundamental mode shape function does not suffer influence due to fluid presence. So, it is assumed that the deformed shape function is identical in both coupled and uncoupled systems (although this kind of behavior does not always happens, as it will be verified later). The same problem occurs in respect to the coupled frequency. This parameter is also needed for calculation of the generalized added mass. However, this frequency is also an unknown parameter of the problem. But, as mentioned before, it is possible to find the system's frequency solution with an imposed shape function. To simplify the mathematical operations involved in calculating the generalized added mass, which leads to a great computational effort, a polynomial approximation to the fundamental exact mode shape is adopted. This leads to:

$$\phi_{approx.}(y) = -0.6457 \left(\frac{y}{H}\right)^3 + 1.6082 \left(\frac{y}{H}\right)^2 + 0.037 \left(\frac{y}{H}\right) - 0.0016 \quad (38)$$

For \tilde{M} and \tilde{K} , the exact deformed shape defined previously will be adopted. Special attention should be given to use of polynomial approximations in parameter \tilde{K} , which involves second order derivatives of $\phi(y)$ in its formulation. It should be noted that curves of polynomial approximation can produce unsatisfactory results for higher order derivatives of a particular function. Figure 6 compares the results obtained for the exact shape function and the polynomial approximation.

The equation for fundamental frequency solution is given by:

$$\omega = \sqrt{\tilde{K}/\tilde{M}_{total}} = \sqrt{\frac{5.41 \times 10^6}{5.00 \times 10 + \int_0^H \left[\frac{\beta}{\phi_{approx.}(y)} \right] [\phi_{approx.}(y)]^2 dy}} \quad (39)$$

This equation can be rewritten as:

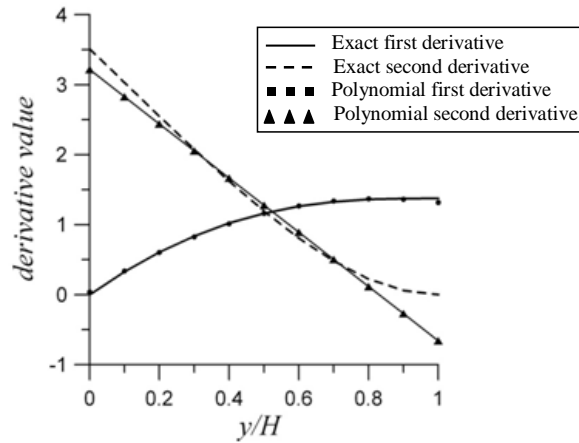


Figure 6: Comparison between exact and polynomial approximation derivatives.

$$5.41 \times 10^6 - \left(5.00 \times 10 + \int_0^H \left[\frac{\beta}{\phi_{approx.}(y)} \right] [\phi_{approx.}(y)]^2 dy \right) \omega^2 = 0 \quad (40)$$

where:

$$\beta = 2\rho \sum_{n=1}^{\infty} \frac{I_n}{\sqrt{\mu_n^2 - \left(\frac{\omega H}{c}\right)^2}} \cos\left(\mu_n \frac{y}{H}\right) \quad (41)$$

The solution of the fundamental frequency equation is related to calculation of β parameter, which depends on the number of terms used in summation. The results obtained using Maple 12 software for evaluation of Eq. (40) are listed in Table 2. These results are compared to a reference value obtained using the Finite Element Method (FEM) for a coupled system.

Table 2: Frequency, number of terms used in summation and processing time.

Number of terms in summation	3	5	10	20	100	FEM (reference)
Frequency (rad/s)	225.5931	223.2586	222.2825	222.0393	221.9615	222.2111
Processing time (s)	2.13	2.54	8.00	63.56	23913.88	-

It can be observed that the number of terms in summation exerts little influence on results, which achieves fast convergence to 222 rad/s . However, processing time is heavily influenced by this parameter. When compared to the reference value, the relative error is close to 0.1%. This frequency represents a decrease of 32.5% when compared to the uncoupled case. The coupled frequency, once established, allows the calculation of the added mass. Thus:

$$\tilde{M}_{fluid} = \int_0^H \left[\frac{\beta}{\phi(y)} \right] [\phi(y)]^2 dy = 5.98 \times 10 \frac{Ns^2}{m} \quad (42)$$

This corresponds to a value greater than the generalized structural mass. Thus, we have the following parameters for the generalized coupled case:

$$\tilde{M} = 5.00 \times 10 + 5.98 \times 10 = 10.98 \times 10 \frac{Ns^2}{m} \quad (43)$$

$$\tilde{K} = 5.41 \times 10^6 \frac{N}{m} \quad (44)$$

It is important to check the value of the compressibility parameter of this problem, which is given by:

$$\frac{\omega H}{c} = \frac{222.00 \frac{1}{s} \times 1m}{1500 \frac{m}{s}} \cong 0.15 \quad (45)$$

This value indicates a close to an incompressible fluid behavior. Thus, it is concluded that satisfactory results would be obtained if the hypothesis of an incompressible fluid was used. In fact, considering this behavior, the achieved frequency would be close to 222.20 rad/s . This value is almost identical to the value obtained for the compressible analysis with a great advantage: that is the elimination of ω in the β parameter.

6.3 Comparative studies between analytical and numerical results (forced vibration)

The equation of motion in free vibration for the structural coupled system can be built after the establishment of generalized parameters. We have:

$$[5.00 \times 10] \ddot{X} + [5.41 \times 10^6] X = 0 \quad (\text{uncoupled}) \quad (46)$$

$$[10.98 \times 10] \ddot{X} + [5.41 \times 10^6] X = 0 \quad (\text{coupled}) \quad (47)$$

For this analysis it will be defined a sine wave excitation applied at the structure's free edge, given by:

$$\tilde{P}(t) = 10^6 \times \sin(50t) \quad (48)$$

Substitution of Eq. (48) in (46) and (47), gives:

$$[5.00 \times 10] \ddot{X} + [5.41 \times 10^6] X = 10^6 \times \sin(50t) \quad (\text{uncoupled}) \quad (49)$$

$$[10.98 \times 10] \ddot{X} + [5.41 \times 10^6] X = 10^6 \times \sin(50t) \quad (\text{coupled}) \quad (50)$$

Solution of the above equation results in:

$$X(t) = -0.028769 \times \sin(328.8931t) + 0.189239 \times \sin(50t) \quad (\text{uncoupled}) \quad (51)$$

$$X(t) = -0.043870 \times \sin(221.9586t) + 0.194748 \times \sin(50t) \quad (\text{coupled}) \quad (52)$$

Velocity and acceleration solutions are given, respectively, by first and second derivatives of Eq. (51) and Eq. (52). Comparison of these functions with coupled and uncoupled finite element solutions is shown on the Fig. 7.

7 Application example 2 – compressible fluid

In this analysis the previous example will be studied with the same geometrical and material properties, except for the Young's modulus, that will be taken as $2.10 \times 10^{12} \text{ MPa}$.

7.1 Uncoupled solution

For the uncoupled solution the following generalized parameter are readily obtained:

$$\tilde{M} = \int_0^H \mu(y) [\phi(y)]^2 dy = \mu \int_0^H [\phi(y)]^2 dy \cong 0.25\mu H = 5.00 \times 10 \frac{Ns^2}{m} \quad (53)$$

$$\tilde{K} = \int_0^H EI(y) \left[\frac{d^2\phi(y)}{dy^2} \right]^2 dy = EI \int_0^1 \left[\frac{d^2\phi(y)}{dy^2} \right]^2 dy \cong 3.09 \frac{EI}{H^3} = 5.41 \times 10^8 \frac{N}{m} \quad (54)$$

$$\omega = \sqrt{\tilde{K}/\tilde{M}} = 3289.34 \frac{\text{rad}}{s} \quad (55)$$

7.2 Coupled solution

The fundamental frequency equation is given by:

$$5.41 \times 10^8 - \left(5.00 \times 10 + \int_0^H \left[\frac{\beta}{\phi_{approx.}(y)} \right] [\phi_{approx.}(y)]^2 dy \right) \omega^2 = 0 \quad (56)$$

The results obtained using Maple 12 software for evaluation of Eq. (56) are listed in Table 3. These results are compared to a reference value obtained using the Finite Element Method (FEM) for a coupled system.

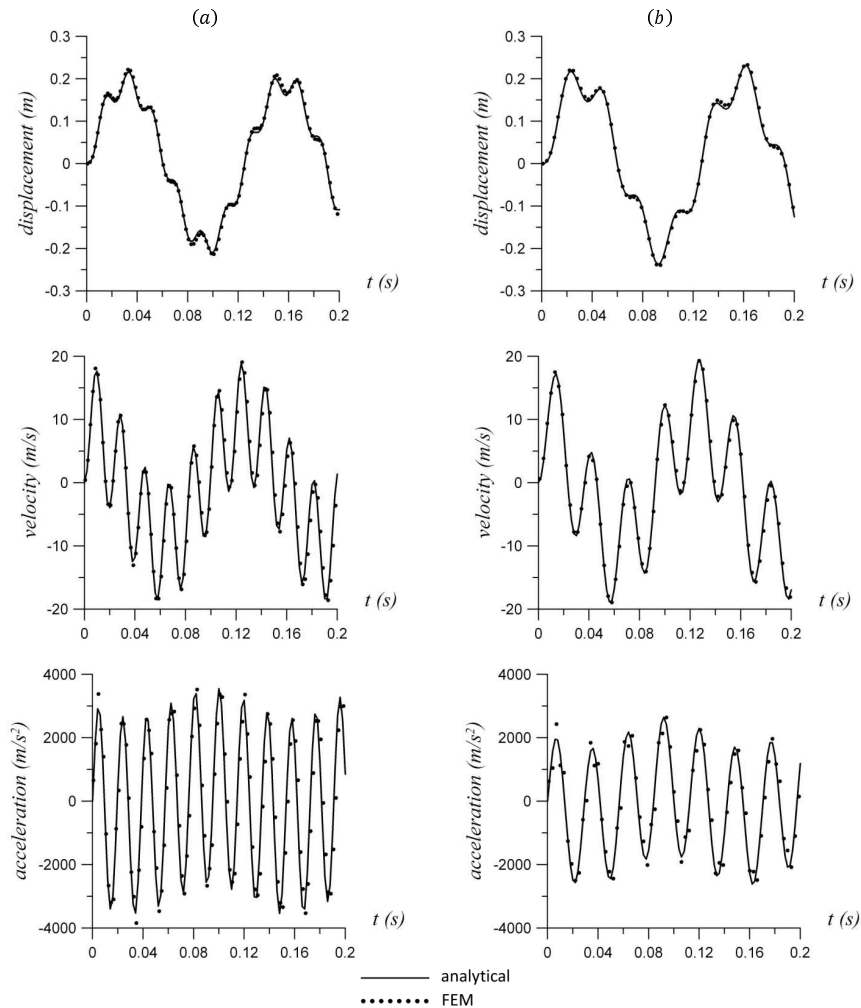


Figure 7: Comparison between FEM response (including all modes) and analytical results. Uncoupled (a) and coupled systems (b).

The above result reaches a fast convergence to values near 1990 rad/s . When compared to the reference value this result indicates a less than 0.2% relative error.

With the fundamental frequency the following generalized parameter is readily obtained:

$$\tilde{M}_{fluid} = \int_0^H \left[\frac{\beta}{\phi(y)} \right] [\phi(y)]^2 dy = 8.67 \times 10 \frac{Ns^2}{m} \quad (57)$$

Table 3: Frequency, number of terms used in summation and processing time.

Number of terms in summation	3	5	10	20	FEM (reference)
Frequency (rad/s)	2006.1886	1995.4492	1990.8595	1989.7070	1986.0520
Processing time (s)	2.10	2.84	7.69	60.15	-

As in the previous analysis, this value is higher than the structural's generalized mass. It should be noted that this fluid added mass is greater than the one obtained in the incompressible case, indicating the effect of a higher compressibility parameter. The added mass produced a 39.5% reduction of the fundamental frequency. In the incompressible analysis this reduction was of 32.5%. These results indicate that fluid compressibility must not be neglected, and that higher fluid added masses are expected with the increase of this parameter, given by:

$$\frac{\omega H}{c} = \frac{1990.00 \frac{1}{s} \times 1m}{1500 \frac{m}{s}} \cong 1.33 \quad (58)$$

Equation (58) indicates a compressible fluid behavior. Treating this problem with an incompressible hypothesis could lead to considerable errors. In fact, the fundamental frequency obtained using an incompressible fluid model would result in 2221.00 *rad/s* (11.6% higher than the one obtained using a compressible fluid model).

7.3 Comparative studies between analytical and numerical results (forced vibration)

The following structural responses results from a sine wave $\tilde{P}(t) = 10^6 \times \sin(450t)$ excitation:

$$X(t) = -0.000258 \times \sin(3288.9312t) + 0.001884 \times \sin(450t) \quad (\text{uncoupled}) \quad (59)$$

$$X(t) = -0.000441 \times \sin(1988.9737t) + 0.001948 \times \sin(450t) \quad (\text{coupled}) \quad (60)$$

Comparison of these functions and its derivatives with finite element solutions is shown on Fig. 8.

8 Application example 3 – concrete gravity dam

In this example a concrete gravity dam with geometrical and material properties given by Fig. 9 and Table 4 will be analyzed (FERC, 2002). However, the analytical generalized procedure will not be used in this analysis. Analytical treatment of these parameters is a complex task, since this structure's geometry is irregular and the fundamental mode shape occurs in both directions (varying both in *x* and *y*). Instead it will be used a semi-analytical procedure, where the uncoupled generalized parameters

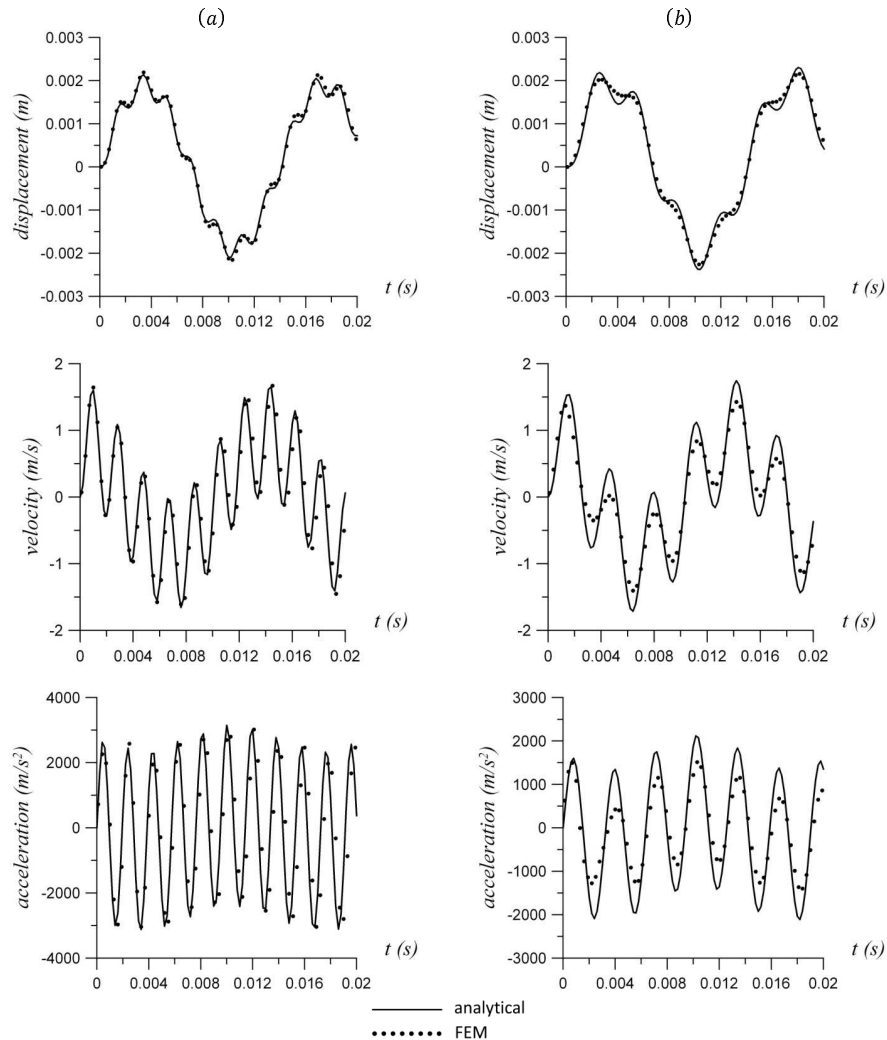


Figure 8: Comparison between FEM response (including all modes) and analytical results. Uncoupled (a) and coupled systems (b).

are going to be obtained from an uncoupled finite element analysis. These results will be introduced in the frequency equilibrium equation, for evaluation of the fundamental coupled frequency.

The generalized parameters obtained in the uncoupled finite element analysis are listed on Table 5. Additionally Eq. (61) indicates a polynomial approximation to the uncoupled fundamental mode shape function. These parameters along with this function are used in the frequency equation, for solution

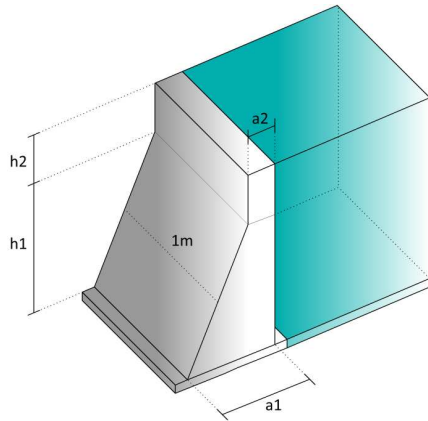


Figure 9: System representation.

Table 4: Geometrical and material properties.

a1	30.48 m
a2	4.57 m
h1	41.45 m
h2	7.32 m
Transverse Young's Modulus (E)	2.10 x 10 ⁴ MPa
Structural mass density (ρ_e)	2000 kg/m ³
Fluid mass density (ρ_f)	1000 kg/m ³
Fluid sonic velocity (c)	1500 m/s

of the coupled system fundamental frequency.

Table 5: Generalized parameters – fundamental mode uncoupled analysis.

Generalized Mass ($\frac{Ns^2}{m}$) \tilde{M}	Generalized Stiffness ($\frac{N}{m}$) \tilde{K}	Earthquake Participation Factor ($\frac{Ns^2}{m}$) \tilde{L}
1.0164 × 10 ⁵	2.1085 × 10 ⁸	2.4086 × 10 ⁵

$$\phi_{approx.}(y) = 0.10851 \left(\frac{y}{H}\right)^4 + 0.61270 \left(\frac{y}{H}\right)^3 + 0.07918 \left(\frac{y}{H}\right)^2 + 0.20411 \left(\frac{y}{H}\right) + 0.00105 \quad (61)$$

The uncoupled fundamental frequency of this system is given by: $\omega = \sqrt{\tilde{K}/\tilde{M}} \cong 45.55 \frac{rad}{s}$.

These parameters can be readily substituted in the frequency equation. Results are shown on Table 6.

From Table 6 it can be observed that the coupled frequency converges to a value near 32.90 rad/s. Comparison with the reference value indicates a 1% relative error. This added mass produced a 27.8% reduction of the fundamental frequency. This generalized parameter is given by:

$$\tilde{M}_{fluid} = \int_0^H \left[\frac{\beta}{\phi(y)} \right] [\phi(y)]^2 dy = 0.9339 \times 10^5 \frac{Ns^2}{m} \quad (62)$$

Verification of the compressibility parameter indicates a compressive behavior for this analysis:

Table 6: Frequency, number of terms used in summation and processing time.

Number of terms in summation	3	5	10	20	FEM (reference)
Frequency (rad/s)	33.4910	33.0988	32.9259	32.8822	33.2462
Processing time (s)	1.23	1.88	6.80	46.81	-

$$\frac{\omega H}{c} = \frac{32.90 \frac{1}{s} \times 48.77 m}{1500 \frac{m}{s}} \cong 1.07 \quad (63)$$

The fluid added mass corresponds to approximately 92% of the structural mass. If this mass is included in the finite element model, representation of the coupled effects in the fundamental mode could be produced without the need of the reservoir. It should be noticed the different behavior between the structural and the fluid added mass. The first one is related to displacements in both directions (x and y). However, the fluid mass is related only to horizontal displacements given by $\phi(y)$, since it is assumed that hydrodynamic pressures develop only due to horizontal accelerations. When the model participation in the y direction is minimal and there is no variation of the mode shape in the transverse direction, then the entire model could be approximated by a single function for all generalized parameters, including the fluid added mass. This is exactly what happened in the previous examples.

For determination of the additional masses that will be inserted in the model, it will be necessary to calculate the β parameter. However calculation is needed only on the exact node locations where these masses are going to be inserted. Consider, as an example, the finite element model illustrated on Fig. 10. Added masses will be placed in 24 nodes along the dam's upstream face. The main objective is to replace the integral given in Eq. (62) by a discrete product of masses and related displacements. Table 7 indicates the calculation procedure.

After the inclusion of the added masses a fundamental modal analysis is required. This will provide the coupled frequency as well as the new deformed shape of the system. It should be noticed that these masses are related only to the fundamental mode of vibration. Figure 11 indicates a comparison between deformed shape results. One of the curves is a representation of transversal displacements x along the dam's height (in this problem defined as U_x). The other one indicates the total displacement, including both directions (x and y , in this problem defined as U_{sum}). We are assuming that fluid added masses should participate only in the transverse direction, but in the first approach the vertical displacements on the dam's upstream face are being neglected (Table 7). From Fig. 11 it can be noticed that this first approach might lead to poor results, since in the finite element model these masses will participate in both directions. Another option, that will provide much better results, is to introduce a modification in column (c), given by:

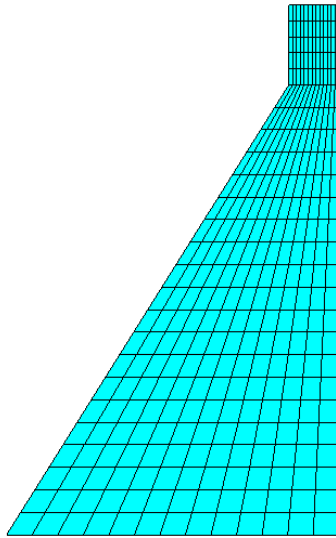


Figure 10: Finite element model.

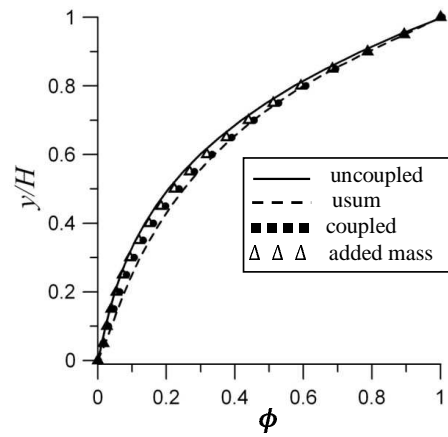


Figure 11: Deformed shape results.

Table 7: Added mass calculation procedure – first procedure (neglecting vertical displacements).

(a) Node	(b) Elevation (m)	(c) $\phi(y)$	(d) Pressure ¹ (normalized) P_{norm}	(e) Nodal tributary area (m ²) A_{node}	(f) Nodal mass ² (10 ⁶ Ns ² /m) M_{node}
48	2.0726	0.0099	0.1347	2.0726	1.3735
49	4.1453	0.0194	0.1358	2.0726	0.7093
50	6.2179	0.0297	0.1373	2.0726	0.4679
51	8.2906	0.0411	0.1392	2.0726	0.3420
.
.
.

¹normalized pressure = $p/(\rho_f \ddot{X}H) = \beta/(\rho_f H)$

²nodal mass = $(d)/(c) \times A_{node} \times \rho_f H$

$$\phi(y) \longrightarrow \alpha(y) = \frac{[U_{sum}(y)]^2}{U_x(y)} \quad (64)$$

This proposed modification takes in account displacements in both directions, and will result exactly

on a product of nodal masses with transverse displacements U_x . Table 8 indicates some sample results for this second procedure.

Table 8: Added mass calculation procedure – second procedure (including vertical displacements).

(a) Node	(b) Elevation (m)	(c) ϕ (y)	(d) Pressure¹ (normalized) P_{norm}	(e) Nodal tributary area (m²) A_{node}	(f) Nodal mass² (10⁶Ns²/m) M_{node}
48	2.0726	0.0313	0.1347	2.0726	0.4350
49	4.1453	0.0606	0.1358	2.0726	0.2264
50	6.2179	0.0868	0.1373	2.0726	0.1598
51	8.2906	0.1107	0.1392	2.0726	0.1271
.
.
.

$$^1\text{normalized pressure} = p / (\rho_f \ddot{X} H) = \beta / (\rho_f H)$$

$$^2\text{nodal mass} = (d)/(c) \times A_{\text{node}} \times \rho_f H$$

Frequencies obtained in both procedures are given in Table 9. It should be noticed that results obtained from the second approach converges to the previously determined coupled frequency. This is exactly what one should expect, since the added masses act as a replacement of Eq. (62).

Table 9: Results comparison between proposed procedures and reference value.

Procedure	first	second	FEM (reference)
Frequency (rad/s)	30.67	32.78	33.25
Relative error (%)	7.76	1.41	-

It can be noticed that the second approach provides much better results when compared to the first procedure. In this analysis vertical displacements can highly influence the fundamental frequency of the system. The differences between the uncoupled and usum curves in Fig. 11 clarify the effect of the vertical component of displacement. This figure also indicates that the fluid added mass approximates the deformed shape to the coupled solution result. If no further refinement is required, then the analysis

could be concluded in this step, with the second procedure added mass solution acting as the coupled system.

8.1 Comparative studies between analytical and numerical results (forced vibration)

In this analysis results from a coupled and uncoupled finite element models are compared to the proposed procedure. The main objective is to verify the dynamic response and the stress field in both approaches during a seismic excitation produced by the north-south component of El Centro earthquake - 1940 (Fig. 12). An excitation time windows of one second is used to simulate this horizontal ground displacement.

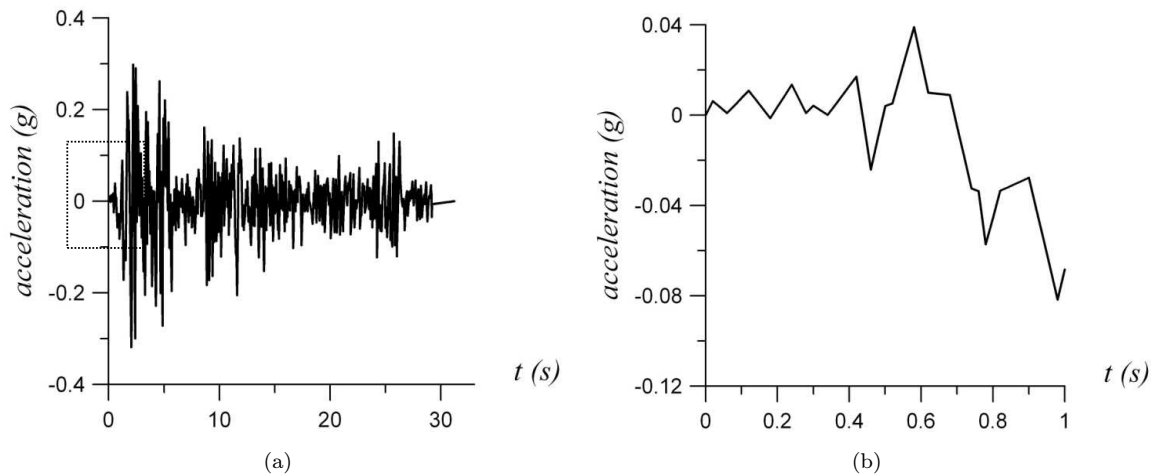


Figure 12: Full record (a) and analysis time window (b) of the north south component of El Centro Earthquake.

The uncoupled equation of motion for this problem is readily obtained with the use of Table 5 parameters. Thus:

$$\left[1.0164 \times 10^5\right] \ddot{X} + \left[2.1085 \times 10^8\right] X = -\ddot{u}_g(t) \times 2.4086 \times 10^5 \quad (\text{uncoupled}) \quad (65)$$

where $\ddot{u}_g(t)$ indicates the horizontal component of ground motion produced by the earthquake. Equation (65) assumes that only translational contributions are involved in the equilibrium equation. However, it should be noticed that this assumption is not entirely right. This equation is solved for the earthquake input using a fourth order Runge-Kutta numerical integration routine. Figure 13a illustrates the dynamic response for the uncoupled solution. Results indicate that this solution leads

to slightly higher displacements when compared to a finite element model response on the fundamental mode shape. Additionally it can be observed on Fig. 13b a comparison between the fundamental solution with a dynamic response including all mode shapes.

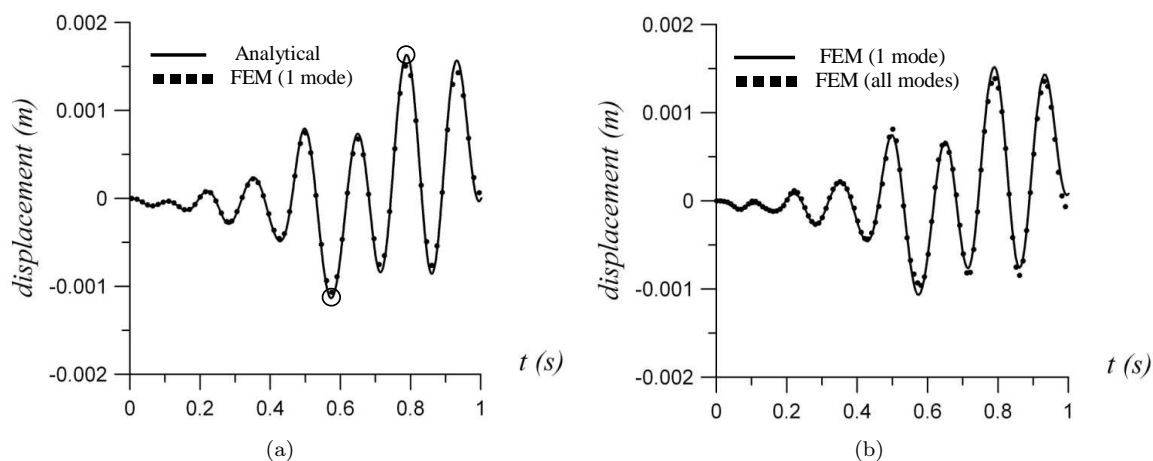


Figure 13: Comparison between analytical and finite element response for the uncoupled system. Analytical and finite element fundamental response (a). Finite element fundamental response and finite element solution including all modes (b).

The above figure indicates that seismic response suffers a significant influence from the fundamental mode shape. Thus, using a fundamental mode analytical approach, with generalized parameters obtained from a finite element analysis provides satisfactory results for the uncoupled case. Equation (65) can be evaluated for other seismic excitations using a numerical integration procedure. This will provide faster results and will allow the prediction of maximum structural responses.

Effective earthquake forces and stress distribution can be readily evaluated once the displacements are known. But there is no need for a time-history evaluation, since peak displacements can be noticed clearly on Fig. 13a. The minimum response value occurs at $t = 0.579s$. And the maximum response occurs at $t = 0.789s$. Figures 14 through 16 illustrate the stress distribution for those peak responses, including the fundamental and the full mode solutions.

The coupled equation of motion for this problem is readily obtained with the use of Table 5 parameters together with the generalized fluid added mass, given by Eq. (62). Thus:

$$\left[1.9503 \times 10^5\right] \ddot{X} + \left[2.1085 \times 10^8\right] X = -\ddot{u}_g(t) \times 4.2187 \times 10^5 \quad (\text{coupled}) \quad (66)$$

where it should be noticed that both the generalized added mass and the generalized excitation now have additional terms that represent the coupling effects. The new generalized added mass is given by

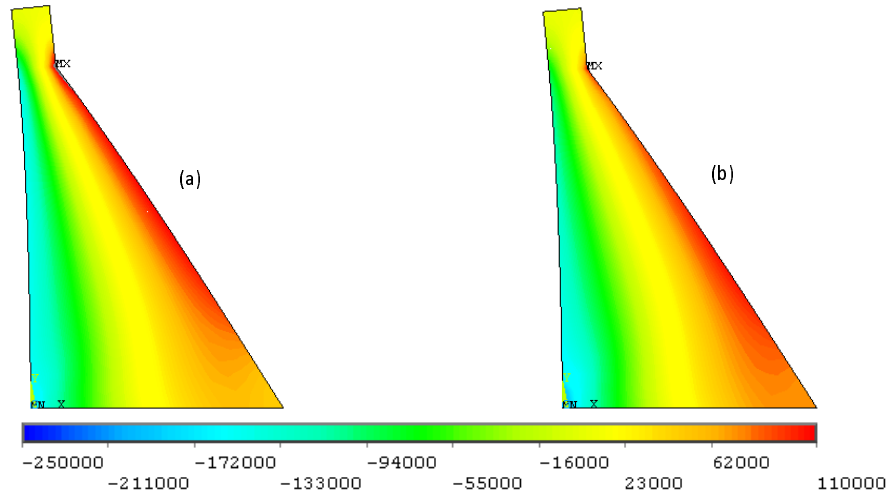


Figure 14: Vertical normal stress distribution for finite element fundamental (a) and full mode solution (b) at $t = 0.579s$. Uncoupled analysis. Stresses in Pa.

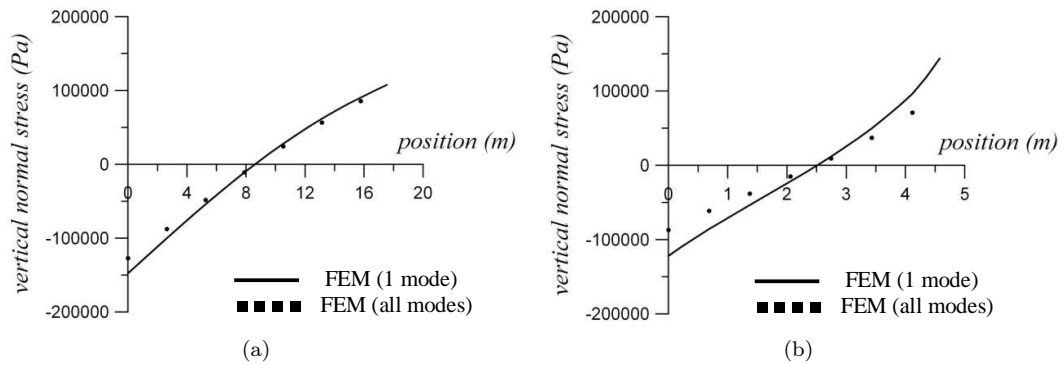


Figure 15: Vertical normal stress distribution at elevations: 20.7264m (a) and 41.4528m (b) at $t = 0.579s$.

the sum of the structural mass with the fluid added mass. And the generalized excitation is given by the sum of the previous parameter with the following term:

$$\tilde{L}_{fluid} = \sum M_{node} \times U_x(y) = 1.8101 \times 10^5 \frac{Ns^2}{m} \tag{67}$$

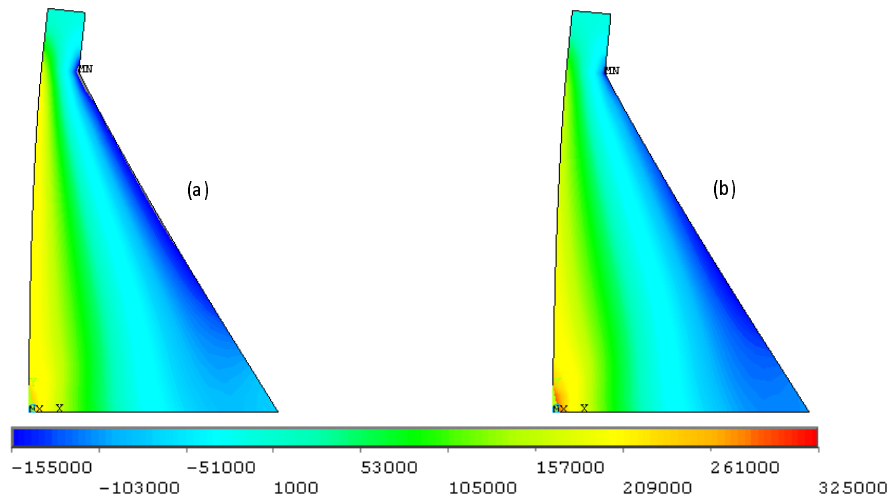


Figure 16: Vertical normal stress distribution for finite element fundamental (a) and full mode solution (b) at $t = 0.789s$. Uncoupled analysis. Stresses in Pa.

which represents the additional mass that participates on the horizontal excitation. Figure 17 illustrates the dynamic response for the coupled solution.

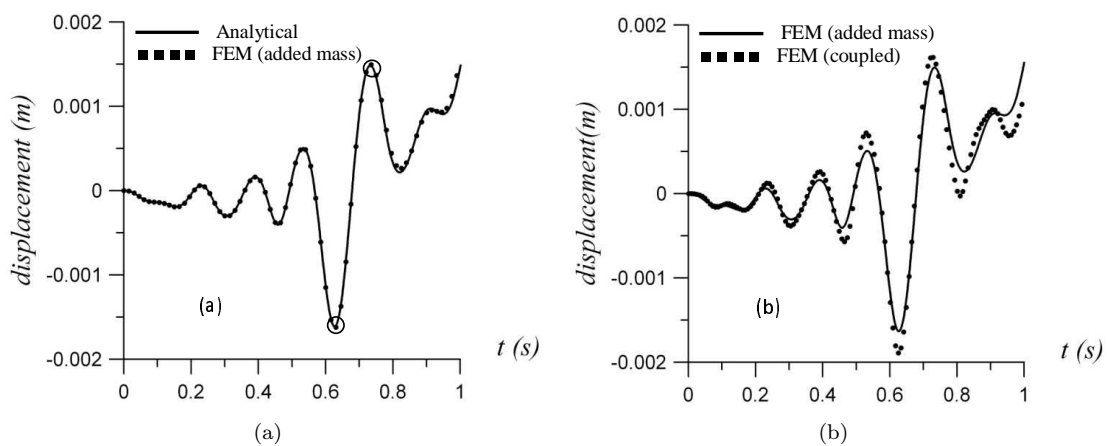


Figure 17: Comparison between analytical and finite element response for the coupled system. Analytical and finite element added mass model fundamental response (a). Finite element added mass model fundamental response and coupled solution including all modes (b).

Figure 17 indicates that seismic response suffers a significant influence from the fundamental mode shape. Thus, using a fundamental mode analytical approach, with generalized parameters obtained from a finite element analysis provides satisfactory results for the coupled case as well. However, it should be noticed that these results have an inferior quality when compared to the uncoupled analysis results.

Effective earthquake forces and stress distribution can be readily evaluated once the displacements are known. But there is no need for a time-history evaluation, since peak displacements can be noticed clearly on Fig. 17a. The minimum response value occurs at $t = 0.627s$. And the maximum response occurs at $t = 0.732s$. Figures 18 and 19 illustrate the stress distribution for those peak responses, including the added mass fundamental and the full mode solutions.

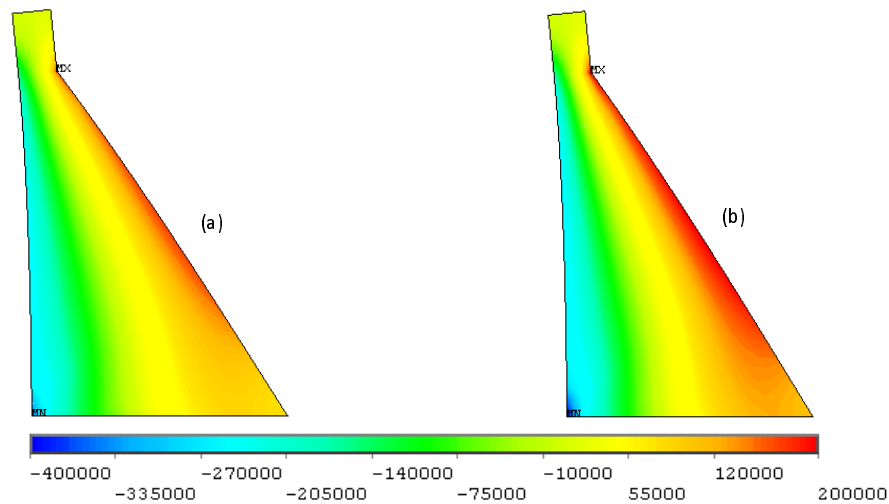


Figure 18: Vertical normal stress distribution for finite element added mass fundamental (a) and full mode solution (b) at $t = 0.627s$. Coupled analysis. Stresses in Pa.

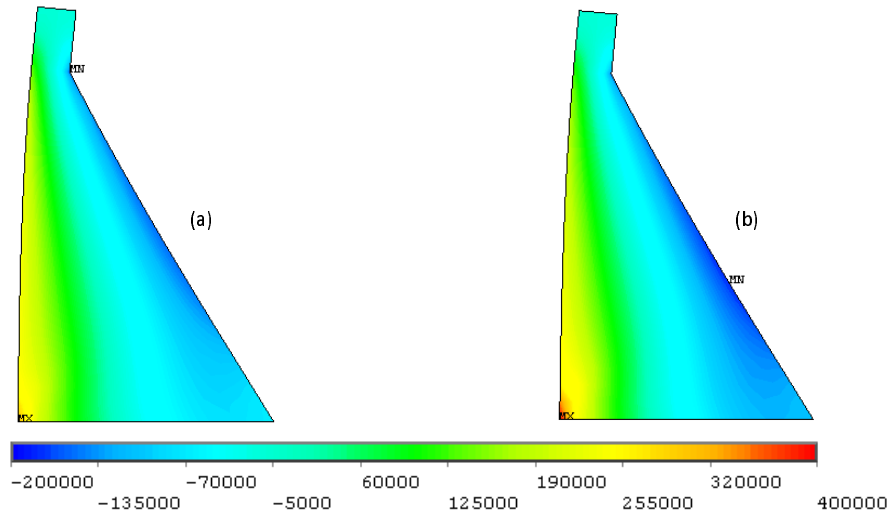


Figure 19: Vertical normal stress distribution for finite element added mass fundamental (a) and full mode solution (b) at $t = 0.732s$. Coupled analysis. Stresses in Pa.

9 Conclusions

A semi-analytical procedure for solution of coupled problems in which a flexible boundary moves into an acoustic fluid domain was presented. On the mathematical development it was proven that hydrodynamic pressures acting on the fluid-structure interface are proportional to the boundary acceleration. This observation provided a link between the structural and fluid systems. A frequency equation was established, being dependent on both the frequency and mode shape of the coupled system. This equation leads to a problem with two unknowns and therefore a solution cannot be found without the previous assumption of one of these parameters. For the mode shape it was adopted the fundamental deformation, leading to problems where frequencies and responses of the first mode were solved. This technique was first introduced to simple problems, where generalized parameters could be easily developed. Complete analytical solutions were found, with results indicating an excellent agreement with coupled results, which considered all modes of vibration. Coupled frequencies had inferior values when compared to uncoupled system results. This provided a conclusion that additional fluid masses were coupled to the structural system. It was also verified that fluid compressibility cannot be neglected on certain analysis, since this parameter provides an additional fluid mass when compared to an incompressible fluid behavior. Therefore, treating a compressible fluid as incompressible will lead to higher coupled frequency values and consequently reduced fluid added masses.

On the second part of this paper the procedure was extended to a more complex geometry. The analysis was developed on a concrete gravity dam, subjected to a seismic excitation. For this analysis

the full analytical solution was replaced by a semi-analytical procedure, in which the generalized parameters for the uncoupled analysis were obtained from a finite element model of this geometry. These parameters were readily substituted in the frequency equation, which provided the coupled frequency, the added mass and an analytical equation of motion. Results indicated a good agreement between the semi-analytical frequency and the coupled value. Later these added fluid masses were introduced on a finite element model and a dynamic analysis considering only the first mode was performed. Stress distribution on this model was compared to a coupled system including all modes. It was shown that the first model provides an approximate solution to the dynamic response, which is highly influenced by the fundamental mode. The great advantage of the added mass procedure is that there is no need to model the reservoir system. Thus this provides a useful resource for finite element computer codes without fluid-structure analysis capabilities. However it should also be noticed that coupled models are more time consuming when compared to uncoupled models. Another great advantage of this procedure is that it provides an analytical equation of motion once the generalized parameters are known. This provides a very efficient tool for estimating maximum structural responses under all sorts of excitations. For simple geometries a full analytical solution can be established, providing coupled frequencies and responses for a given mode shape. So this procedure could also be extended to account for participation of higher modes in the structural response.

Acknowledgements

The authors are grateful for the financial support provided by CAPES and CNPq scholarships.

References

- [1] Westergaard, H.M., Water pressures on dams during earthquakes. *Transactions ASCE*, **98**, pp. 418–472, 1933.
- [2] Zienkiewicz, O.C. & Newton, R.E., Coupled vibrations of a structure submerged in a compressible fluid. *International Symposium on Finite Element Techniques*, Stuttgart, Germany, 1969.
- [3] Sharan, S.K., Finite Element analysis of unbounded and incompressible fluid domains. *International Journal for Numerical Methods in Engineering*, **21**, pp. 1659–1669, 1985.
- [4] Küçükarslan, S., Dam-reservoir interaction for incompressible-unbounded fluid domains using an exact truncation boundary condition. *16th ASCE Engineering Mechanics Conference*, University of Washington: Seattle, p. 9, 2003.
- [5] Silva, S.F. & Pedroso, L.J., Estudo analítico-numérico do campo de pressões e da massa adicional em barragens durante terremotos. Technical Report RTP-SFS2, UnB-FT/ENC, Brasília, 2005.
- [6] Chopra, A.K., Earthquake behavior of dam-reservoir systems. *Journal of Engineering Mechanics, ASCE*, **94**, pp. 1475–1499, 1968.
- [7] Chopra, A.K., *Earthquake Response of Concrete Gravity Dams*. UCB/EERC-70/01, Earthquake Engineering Research Center, University of California: Berkeley, p. 20, 1970.
- [8] Fenves, G.L. & Chopra, A.K., *EAGD-84: A Computer Program for Earthquake Analysis of Concrete Gravity Dam*. UCB/EERC-84/11, Earthquake Engineering Research Center, University of California: Berkeley, p. 92, 1984.

- [9] Fenves, G.L. & Chopra, A.K., *Earthquake Analysis and Response of Concrete Gravity Dams*. UCB/EERC-84/10, Earthquake Engineering Research Center, University of California: Berkeley, p. 228, 1984.
- [10] Saini, S., Bettess, P. & Zienkiewicz, O.C., Coupled hydrodynamic response of concrete dams using Finite and Infinite Elements. *Earthquake Engineering and Structural Dynamics*, **6**, pp. 363–374, 1978.
- [11] Chopra, A.K. & Chakrabarti, P., Earthquake analysis of concrete gravity dams including dam-fluid-foundation rock interaction. *Earthquake Engineering and Structural Dynamics*, **9**, pp. 363–383, 1981.
- [12] Hall, J.F. & Chopra, A.K., Two dimensional dynamic analysis of concrete gravity and embankment dams including hydrodynamic effects. *Earthquake Engineering and Structural Dynamics*, **10**, pp. 305–332, 1982.
- [13] Fenves, G. & Chopra, A.K., Effects of reservoir bottom absorption and dam-water-foundation rock interaction on frequency response functions for concrete gravity dams. *Earthquake Engineering and Structural Dynamics*, **13**, pp. 13–31, 1985.
- [14] Fok, K.L. & Chopra, A.K., *Earthquake Analysis and Response of Concrete Arch Dams*. UCB/EERC-85/07, Earthquake Engineering Research Center, University of California: Berkeley, p. 207, 1985.
- [15] Lotfi, V., Roesset, J.M. & Tassoulas, J.L., A technique for the analysis of the response of dams to earthquakes. *Earthquake Engineering and Structural Dynamics*, **15**, pp. 463–490, 1987.
- [16] Ribeiro, P.M.V., *Uma Metodologia Analítica para Avaliação do Campo de Tensões em Barragens de Concreto Durante Terremotos*, *Dissertação de Mestrado em Estruturas e Construção Civil, Publicação E.DM-003A/06*. Departamento de Engenharia Civil e Ambiental, Universidade de Brasília: Brasília, DF, p. 162, 2006.
- [17] USBR (United States Bureau of Reclamation), *Design of gravity dams*. United States Department of the Interior - Bureau of Reclamation, 1976.
- [18] Chopra, A.K., Earthquake resistant design of concrete gravity dams. *Journal of the Structural Division, ASCE*, **104(ST6)**, pp. 953–971, 1978.
- [19] Silva, S.F., *Interação Dinâmica Barragem-Reservatório: Modelos Analíticos e Numéricos*, *Tese de Doutorado em Estruturas e Construção Civil, Publicação E.TD-05A/07*. Departamento de Engenharia Civil e Ambiental, Universidade de Brasília: Brasília, DF, p. 220, 2007.